Article

Cite This: *Biomacromolecules* XXXX, XXX, XXX−XXX

pubs.acs.org/Biomac

Comparison of Photo Cross Linkable Gelatin Derivatives and Initiators for Three-Dimensional Extrusion Bioprinting

Thomas J. Tigner,[†] Satyam Rajput,[†] Akhilesh K. Gaharwar,[†,‡] and Daniel L. Alge*[,†,‡]

[†]Department of Biomedical Engineering, College of Engineering, and [‡]Department of Materials Science and Engineering, College of Engineering, Texas A&M University, College Station, Texas 77840, United States

Supporting Information

ABSTRACT: The objective of this study was to evaluate the utility of gelatin−norbornene (GelNB), which is cross-linkable via thiol−ene click chemistry, and the photoinitiator lithium phenyl-2,4,6 trimethylbenzoylphosphinate (LAP) for 3D bioprinting. These materials were compared to two widely used materials, gelatin-methacryloyl (GelMA) and 2-hydroxy-4′-(2-hydroxyethoxy)-2-methylpropiophenone (I2959). Characterization of photocuring kinetics revealed that LAP markedly improved the kinetics compared to I2959, which improved stability and print fidelity. Additionally, GelNB exhibited improved photocuring kinetics, improved stability, and decreased filament spreading compared to GelMA. However, inks containing GelMA yielded at lower stress, were more easily extruded, and produced smoother filaments. NIH 3T3 fibroblasts exhibited high viability in printed constructs, regardless of the gelatin derivative or photoinitiator used. Overall, these results support the selection of LAP over I2959 and suggest that GelNB could be a useful alternative to GelMA, although further work is needed to optimize GelNB extrusion.

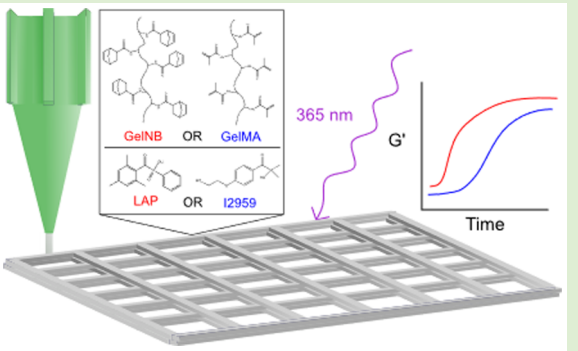

INTRODUCTION

The emergence of three-dimensional (3D) bioprinting is fueling a revolution in the design of functional tissue replacements. Bioprinting employs additive manufacturing to controllably deposit formulations of biomaterials and cells, so-called bioinks, in 3D space, enabling efficient and high-throughput fabrication of complex tissue-mimetic structures.[1−3] Among a variety of bioprinting techniques, extrusion bioprinting is advantageous for its compatibility with viscous bioinks and high cell seeding densities as well as its affordability and accessibility.[3]

Gelatin modified with methacryloyl moieties (GelMA) has been commonly employed as a macromer component in extrudable bioink formulations.[4−7] GelMA's naturally derived amino acid sequence affords bioinks with advantageous enzymatic degradability and integrin binding domains.[8,9] Moreover, synthetic modification with methacryloyl moieties enables chemical cross-linking via a chain-growth polymerization reaction to produce hydrogel matrices with controllable mechanical properties.[8,10,11] In bioprinting applications, chemical cross-linking has been applied postfabrication to permanently stabilize 3D printed constructs as well as during fabrication to preserve spatial resolution.[6,12−14] Nevertheless, methacryloyl chemistry is not an ideal approach to preserve spatial resolution. Specifically, because of its chain-growth polymerization mechanism, GelMA cross-linking is slow and inhibited by dissolved oxygen, which acts as a radical scavenger.[15] While oxygen inhibition can be overcome by increasing UV light dosage,[16] this approach is undesirable due to potential stress and damage to cells.[17,18] To preserve spatial resolution during printing, researchers have instead relied on higher GelMA concentrations[6,14] (which are known to adversely impact cell viability[19]) or on more complex bioink formulations, containing viscosity-modifying additives.[20−24]

Recently, gelatin modification with norbornene moieties (GelNB) has been described, providing a foundation for a new generation of thiol−ene cross-linkable gelatin-based bioinks that overcome the limitations of GelMA.[25−29] The radical-mediated thiol−ene click reaction proceeds through a step-growth polymerization mechanism. In the presence of thiols and dissolved oxygen, thiyl radicals preferentially form during chain transfer, imparting oxygen insensitivity during reaction progression.[30,31] Additionally, norbornene moieties offer the fastest chain-transfer kinetics of all previously investigated alkenes due to relief of its highly strained double bond.[30] Thiol−ene chemistry has been widely applied in the fabrication of synthetic hydrogel systems[32] and, more recently, in the chemical cross-linking of natural biomaterials, like alginate and pectin.[33,34] In comparison to chain-growth polymerization mechanisms, thiol−ene chemistry exhibits faster reaction kinetics, improved cell viability, and decreased indications of cellular oxidative stress in both gelling and nongelling

Received: August 30, 2019
Revised: November 15, 2019
Published: November 19, 2019

DOI: 10.1021/acs.biomac.9b01204
Biomacromolecules XXXX, XXX, XXX−XXX

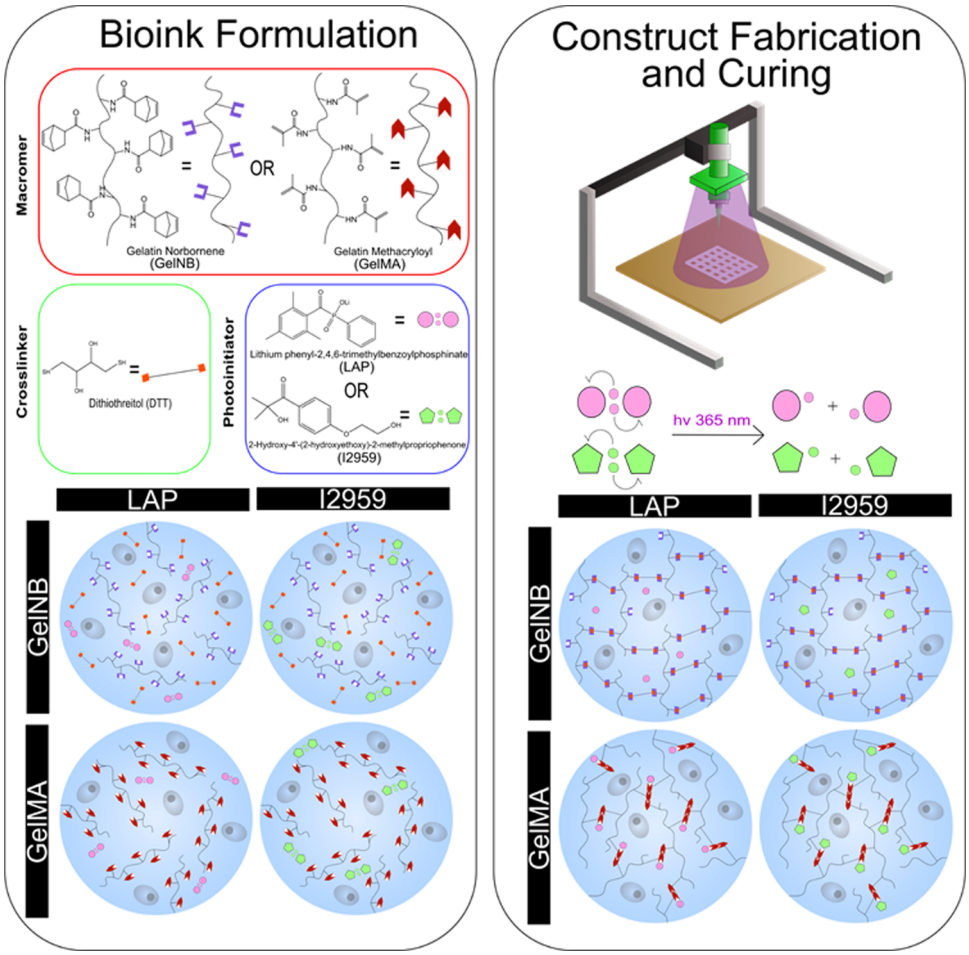

Figure 1. Schematic of bioink formulation and 3D printing. Bioinks were formulated in PBS with 10% w/v GelNB or GelMA as a macromer component and 4.46 mM LAP or I2959 as a photoinitiator component. 3D constructs were fabricated from bioink formulations by using extrusion bioprinting with simultaneous photocuring (365 nm light).

reactions.[35−37] Moreover, thiol−ene chemistry produces relatively homogeneous hydrogel networks with more robust mechanical properties.[38]

Regardless of whether GelMA or GelNB is used, the selection of the photoinitiator species is also important. To date, 2-hydroxy-4′-(2-hydroxyethoxy)-2-methylpropiophenone, commonly known by its trade name Irgacure D-2959 (I2959), has been most often employed because of its cytocompatibility and sufficient cleavage kinetics to facilitate gelation upon exposure to broad-spectrum UV light.[39,40] However, I2959 exhibits peak light absorbance around 280−300 nm and only tail absorbance at more cytocompatible 365 nm light.[39,41] In recent years, lithium phenyl-2,4,6 trimethylbenzoylphosphinate (LAP) has been attracting increased attention. Importantly, LAP exhibits faster radical-cleavage kinetics at 365 nm light compared to I2959, decreasing gelation time in PEG-diacrylate hydrogels.[41] Faster curing could be advantageous in the design of fast-curing bioinks for the preservation of spatial fidelity during fabrication.

Herein, the effects of thiol−ene chemistry and LAP photoinitiation on printed construct fidelity and encapsulated cell viability were assessed. To achieve this, GelNB and LAP were incorporated into bioink formulations and directly compared to GelMA and I2959 (Figure 1). We hypothesized GelNB and LAP would impart faster curing kinetics at lower UV dosages, which would translate to improved construct stability, fidelity, and cell viability.

MATERIALS AND METHODS

Macromer Synthesis and Characterization. GelNB was synthesized by using a protocol adapted from Truong et al.[42] Briefly, anhydrous dichloromethane (Acros Organics) was added to a round-bottom flask purged with nitrogen gas. *N*-Hydroxysuccinimide (Aldrich), 5-norbornene-2-carboxylic acid (Alfa Aesar), and triethylamine (Alfa Aesar) were added to the round-bottom flask at concentrations of 0.684 M, 0.684 M, and 34.2 mM, respectively. The reactants were allowed to dissolve under constant stirring for about an hour before *N*,*N*′-diisopropylcarbodiimide (Alfa Aesar) was added dropwise to the round-bottom flask over the course of about 5 min to a final concentration of 0.684 M. The reaction was allowed to proceed for 24 h under a nitrogen blanket. After 24 h, the reaction solution was filtered by using a Buchner funnel and filter paper to remove the solid urea waste product. The filtered solution was transferred to a Hei-Vap rotary evaporator (Heidolph), and solvent was evaporated to yield the white, waxy product, which used in the next step without further purification.

Type A gelatin from porcine skin (Sigma, 300 g Bloom) and triethylamine were dissolved in dimethyl sulfoxide (VWR International) at 50 °C under constant stirring to final concentrations of 10% w/v and 71 mM, respectively. The white, waxy product from the previous reaction was added to the round-bottom flask to a concentration of 3.34% w/v. After 24 h, the reaction was terminated by the addition of the reaction solution to ×2 the reaction volume of

DOI: 10.1021/acs.biomac.9b01204
Biomacromolecules XXXX, XXX, XXX−XXX

distilled water. The solution was transferred to dialysis membranes with 12−14 kDa MWCO (Spectrum Laboratories), and the product was dialyzed against distilled water at 45 °C. The dialyzed product was then frozen, lyophilized, and stored at −20 °C until later use.

GelMA was synthesized by using a protocol adapted from Shirahama et al.[43] Briefly, type A gelatin from porcine skin was dissolved in 0.25 M carbonate−bicarbonate buffer at 50 °C under constant stirring to a final concentration of 10% w/v. The pH of the solution was adjusted to 9 through the addition of hydrochloric acid (VWR International). 1.0 mL of methacrylic anhydride (Sigma-Aldrich) was added dropwise to the gelatin solution over the course of about 5 min. The reaction was allowed to proceed for 3 h before termination by adjustment of the pH to 7.4 by using hydrochloric acid. The solution was transferred to dialysis membranes with 12−14 kDa MWCO, and the product was dialyzed against distilled water at 45 °C. The dialyzed product was frozen, lyophilized, and stored at −20 °C until later use.

Determination of Macromer Functionalization. GelNB and GelMA were separately dissolved in deuterium oxide (Aldrich). NMR spectra were obtained by using either an INOVA300 system or an INOVA500 system. For GelNB spectra (Figure S1), the intensity of the alkene peaks (6.10 and 5.75 ppm) from norbornene moieties was normalized to the intensity of the methyl peak (0.75 ppm) from valine, leucine, and isoleucine residues in the gelatin backbone. For GelMA spectra (Figure S2), the intensity of the alkene peaks (5.55 and 5.26 ppm) from methacrylol moieties was normalized to the intensity of the methyl peak (0.75 ppm). Equation S1, for the degree of functionalization of GelNB, and eq S2, for the degree of functionalization of GelMA, were formulated according to the methods presented by van Hoorick et al.[27] and modified to reflect the composition of gelatin as reported by Claaßen et al.[44] Three batches of GelNB were synthesized, with functionalizations of 0.235, 0.251, and 0.298 mmol of norbornene per gram of gelatin, and two batches of GelMA were synthesized, with functionalizations of 0.282 and 0.361 mmol of methacryloyl per gram of gelatin.

Biomaterial Ink Formulation. Lyophilized products, photoinitiators, and cross-linker were individually dissolved in phosphate buffered saline (PBS) to prepare concentrated stock solutions. Stocks were subsequently mixed at 40 °C to prepare biomaterial inks at the targeted working concentrations. Biomaterial inks were prepared at a working macromer (GelNB or GelMA) concentration of 10% w/v and photoinitiator (LAP or I2959) concentration of 4.46 mM (corresponding to 0.1% w/v I2959). 1,4-Dithiothreitol (DTT) was added to GelNB biomaterial inks at a thiol−ene ratio of 1:1. Unless otherwise specified, biomaterial inks were mixed at 40 °C and then allowed to physically gel at ambient room temperature (22.5 °C) for about 20−60 min before use in experiments. Stock macromer solutions that were intended to be mixed with cells to form bioinks were dissolved in sterile PBS and exposed to germicidal UV light for at least 30 min. Sterile stock photoinitiator and DTT solutions were prepared via filter sterilization using 0.2 μm syringe filters (VWR).

Rheological Characterization of Biomaterial Inks. All rheological sweeps were conducted on a TA Instruments Discovery HR2 rheometer using acellular, nonsterile biomaterial ink formulations. Strain amplitude and shear rate sweeps were conducted by using a Peltier plate stage and 20 mm parallel plate geometry. Biomaterial inks were heated to about 40 °C to facilitate pipetting. About 115 μL of biomaterial ink was deposited onto the stage by using a variable volume pipette. The gap distance was set to 200 μm, and the samples were trimmed and left to soak at 22.5 °C for at least 10 min. Strain amplitude sweeps were conducted in the range of 1−1000% strain and at a frequency of 1 Hz, and shear rate sweeps were conducted in the range of 0.1−30 s^{-1}.

In situ curing time sweeps were collected by using the rheometer's UV-curing stage and a 20 mm parallel plate geometry. About 55 μL of heated biomaterial ink was deposited onto the stage, and the geometry was lowered to a gap distance of 100 μm. A lower gap distance was used in curing sweeps compared to strain and rate sweeps to ensure uniform light exposure throughout the samples' thicknesses. The samples were trimmed and allowed to soak at 22.5 °C for at least 10 min before initiation of the experiment. All time sweeps were conducted under a shear stress of 1 Pa and a frequency of 1 Hz. For biomaterial inks containing LAP, samples were exposed to 365 nm light at an intensity of 5 mW cm^{-2}, beginning at 30 s and ending at 210 s. For biomaterial inks containing I2959, samples were exposed to 365 nm light at an intensity of 15 mW cm^{-2}, beginning at 30 s and ending at 510 s. A greater light intensity was used in I2959 initiated sweeps to ensure timely curing of the biomaterial inks.

Thermal hysteresis in the physical gelation kinetics of GelMA biomaterial inks was also evaluated via rheology and time sweep measurements. The Peltier plate stage and a 40 mm parallel plate geometry were used. Approximately 375 μL of heated GelMA + LAP and GelMA + I2959 biomaterial inks was deposited on the rheometer's stage. The gap distance was set to 200 μm, and the samples were trimmed. An oscillatory shear stress of 1 Pa was then applied at a frequency of 1 Hz for 3 min at 40 °C, after which the temperature was decreased to 22.5 °C, and measurements were recorded for an additional 60 min.

Construct CAD Modeling and G-Code Generation. All prints were conducted on an Anet-A8 3D printer, modified to facilitate the screw-based extrusion of hydrogels. CAD models were developed in SOLIDWORKS 2018 and saved as STL files. Slic3r was used to adjust print parameters (print speed and extrusion speed) and convert STL files to G-code files, which were uploaded to Repetier-Host v1.1.0 for Mac and used to control the print process. Extrusion speeds were calculated from values in the generated G-code according to eq S3. All prints were conducted by using an 18 gauge nozzle (838 μm i.d.) unless otherwise specified. Photocuring was applied during deposition using a custom UV-curing accessory for the bioprinter, which interfaced about the extruder shaft and exposed constructs to 365 nm light from above.

Print Parameter Optimization. The nozzle diameter was first optimized. Acellular, nonsterile biomaterial inks were loaded into the extruder shaft and extruded through 18 and 20 gauge nozzles. The printability of the inks was qualitatively evaluated according to their propensity to form regular filaments upon extrusion. Nozzle head and extrusion speeds were subsequently optimized. The GelNB + I2959 and GelMA + I2959 biomaterial ink formulations were printed in parallel lines, conducted at print speeds of 5, 10, and 15 mm s^{-1} and extrusion speeds ranging from 2.0 to 4.0 mm s^{-1} in increments of 0.5 mm s^{-1}. (Note: the extrusion speed is the rate at which the plunger in the extruder moves; these extrusion speeds correspond to volumetric extrusion speeds of 28.51−57.01 μL s^{-1} in increments of 5.70 μL s^{-1}.) The deposited extrusion filaments were classified as overextruded, underextruded, or appropriately extruded according to a qualitative evaluation of filament continuity and diameter regularity.

Assessment of Vertical Stability. Acellular, nonsterile biomaterial ink formulations were printed as vertically oriented cylindrical constructs. The CAD file was designed as a hollow cylinder, 10 cm (100 layers) in height with an o.d. of 10 mm and an i.d. of 9.16 mm. Biomaterial ink formulation containing GelNB was printed at a print speed of 10 mm s^{-1} and extrusion speed of 2 mm s^{-1}, while formulations containing GelMA were printed at a print speed of 15 mm s^{-1} and extrusion speed of 3 mm s^{-1} (i.e., 42.77 μL s^{-1}). During printing, biomaterial ink formulations containing LAP were continuously exposed to 365 nm light at an intensity of 5 mW cm^{-2} at the print layer, while biomaterial inks containing I2959 were continuously exposed to 365 nm light at an intensity of 20 mW cm^{-2} at the print layer. Prints were terminated if a noticeably large gap between the print layer and nozzle was observed.

Assessment of *X*−*Y* Print Fidelity and Filament Spreading. Acellular, nonsterile biomaterial ink formulations were printed in a grid pattern. The CAD file was designed as a 6 square by 6 square grid, 1 cm (5 layers) in height. Each square in the grid was designed to be 4.19 mm by 4.19 mm in internal dimensions. All biomaterial ink formulations were printed at a print speed of 15 mm s^{-1} and an extrusion speed of 3 mm s^{-1} (42.77 μL s^{-1}). During printing, biomaterial ink formulations containing LAP were continuously exposed to 365 nm light at an intensity of 5 mW cm^{-2} at the print layer, while biomaterial inks containing I2959 were continuously

DOI: 10.1021/acs.biomac.9b01204
Biomacromolecules XXXX, XXX, XXX−XXX

exposed to 365 nm light at an intensity of 20 mW cm^{-2} at the print layer. Constructs were imaged on a SteREO Discovery.V8 microscope (ZEISS). Images were stitched together by using the "pairwise stitching" plugin for ImageJ. The "Measure" tool was used to determine extrusion diameters, and the "MRI Wound Healing" tool was used to determine void area and circularity. Each measured quantity was normalized to its corresponding theoretical value, assumed to be the internal diameter of the 18 gauge nozzle (838 μm) for extrusion diameter, the void areas of the CAD file (17.5 mm^2) for void area, and the circularity of a perfect square (0.785) for void circularity. Measured quantities were subjected to ordinary one-way ANOVA followed by Tukey's multiple comparison test. Constructs were removed from the glass collecting stage by using a razor blade to assess their handleability.

Cell Culture and Bioink Formulation. NIH 3T3 fibroblasts were cultured in high humidity at 37 °C and 5% CO_2 on tissue culture plastic polystyrene in complete media (Dulbecco's Modified Eagle Media with 10% fetal bovine serum albumin and antibiotic−antimycotic solution (50 U mL^{-1} penicillin, 50 μg mL^{-1} streptomycin)). At the time of construct fabrication, cells were lifted from culture by using 0.05% trypsin. Trypsin was deactivated via addition of ×4 its volume of complete media. Cells were centrifuged at 1400 rpm and room temperature for 4 min. The supernatant was decanted, and the pellet was resuspended in sterile PBS to create a stock cell suspension. This cell suspension was mixed with sterile stock biomaterial ink solutions at 37 °C to create bioink formulations at a working concentration of 2 million cells mL^{-1}. Before loading into the extruder shaft, bioinks were incubated at 4 °C for about 5 min to expedite physical gelation and then allowed to equilibrate at ambient room temperature (22.5 °C).

Assessment of NIH 3T3 Viability in Bioprinted Constructs. NIH 3T3 bioink formulations were loaded into the bioprinter's extruder shaft, and cell-laden constructs were printed in a 2 square by 2 square grid pattern. All formulations were printed at a print speed of 15 mm s^{-1} and an extrusion speed of 3 mm s^{-1} (42.77 μL s^{-1}). LAP-containing formulations were continuously exposed to 365 nm light at an intensity of 5 mW cm^{-2} at the print layer concurrent with printing. By use of the same method, I2959-containing formulations were exposed to light at an intensity of 20 mW cm^{-2} followed by postprocessing exposure to 365 nm light at 100 mW cm^{-2} for 30 s from an OmniCure S2000 lamp (Lumen Dynamics) with an external filter adaptor kit (IGB-Technologies). Constructs were transferred to polystyrene culture dishes, submerged in complete media, and cultured in high humidity at 37 °C and 5% CO_2 with media changed every 2 days. At 1, 3, and 7 days of culture, three constructs of each bioink formulation were removed from the culture and stained with 2 μM Calcein AM (VWR) and 4 μM Ethidium Homodimer (VWR) according to standard protocol. Constructs were imaged on an FV1000 confocal microscope (Olympus). Cells were counted from maximum projection images using the "find maxima" tool in ImageJ, and construct viabilities were calculated therefrom. Construct viability data were subjected to a two-way ANOVA followed by Tukey's multiple comparisons test for simple effects within culture time points. Full constructs were imaged on a SteREO Discovery.V8 microscope using the fluorescence module.

RESULTS AND DISCUSSION

Rheological Characterization of Biomaterial Inks. During extrusion, bioinks should exhibit (1) yielding and viscous deformation under the application of low shear and (2) shear-thinning properties upon increasing shear.[2,23,45] Thus, yielding and shear-thinning character in uncured biomaterial inks containing either GelNB or GelMA and either LAP or I2959 were rheologically evaluated. To evaluate yielding, biomaterial inks were subjected to oscillatory strain amplitude sweeps. All biomaterial inks were physically gelled at room temperature and exhibited yielding at about 100% strain. Interestingly, biomaterial inks containing GelNB exhibited

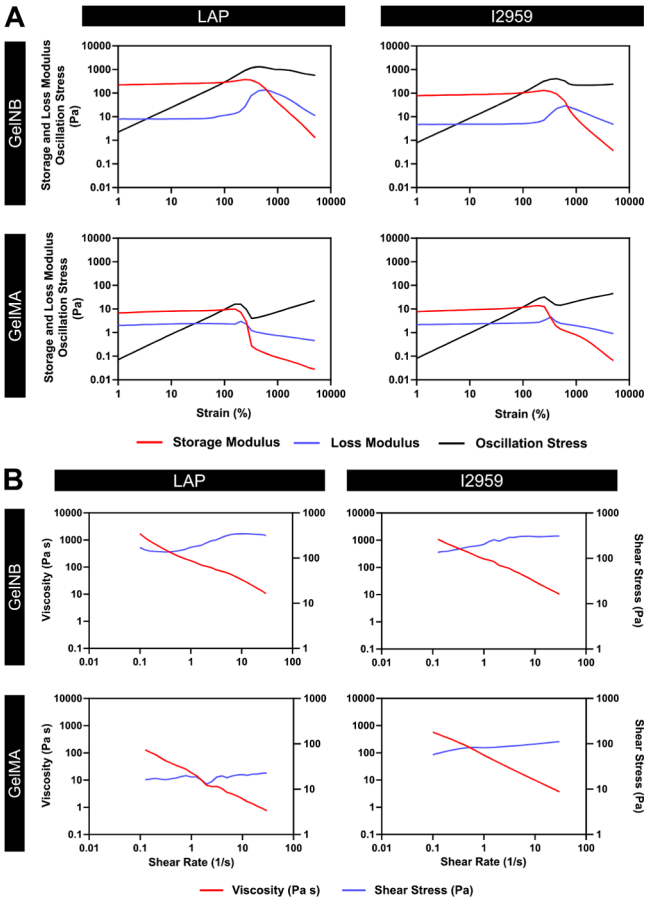

Figure 2. Rheological properties of biomaterial inks prior to UV photocuring. Biomaterial inks formulated from GelNB, GelMA, LAP, and I2959 were subjected to (A) oscillatory strain-amplitude sweeps and (B) shear-rate sweeps.

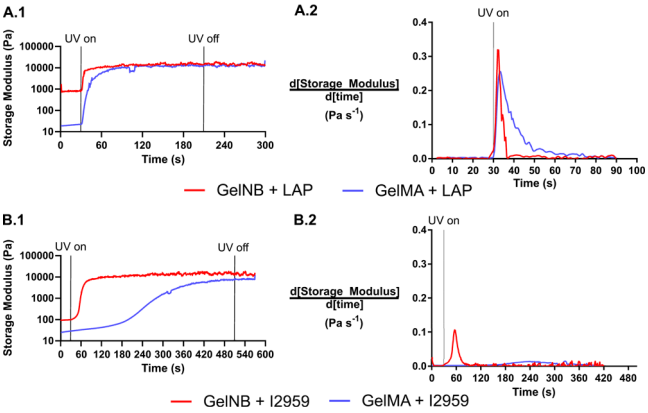

Figure 3. *In situ* UV-curing sweeps of biomaterial inks. (A.1−B.1) Storage modulus was recorded as a function of time (A.2−B.2) and the first derivative was computed. (A) LAP-initiated sweeps were exposed to 365 nm light at an intensity of 5 mW cm^{-2}, and (B) I2959-initiated sweeps were exposed at an intensity of 15 mW cm^{-2}. Biomaterial inks were formulated with 4.46 mM photoinitiator.

storage moduli about an order of magnitude greater than biomaterial inks containing GelMA (Figure 2A). The formation of stronger physical gels in GelNB inks compared to GelMA inks likely indicates that conjugated norbornene moieties disrupt gelatin's native right-handed triple-helix structures less than conjugated methacryloyl moieties.[46]

DOI: 10.1021/acs.biomac.9b01204
Biomacromolecules XXXX, XXX, XXX−XXX

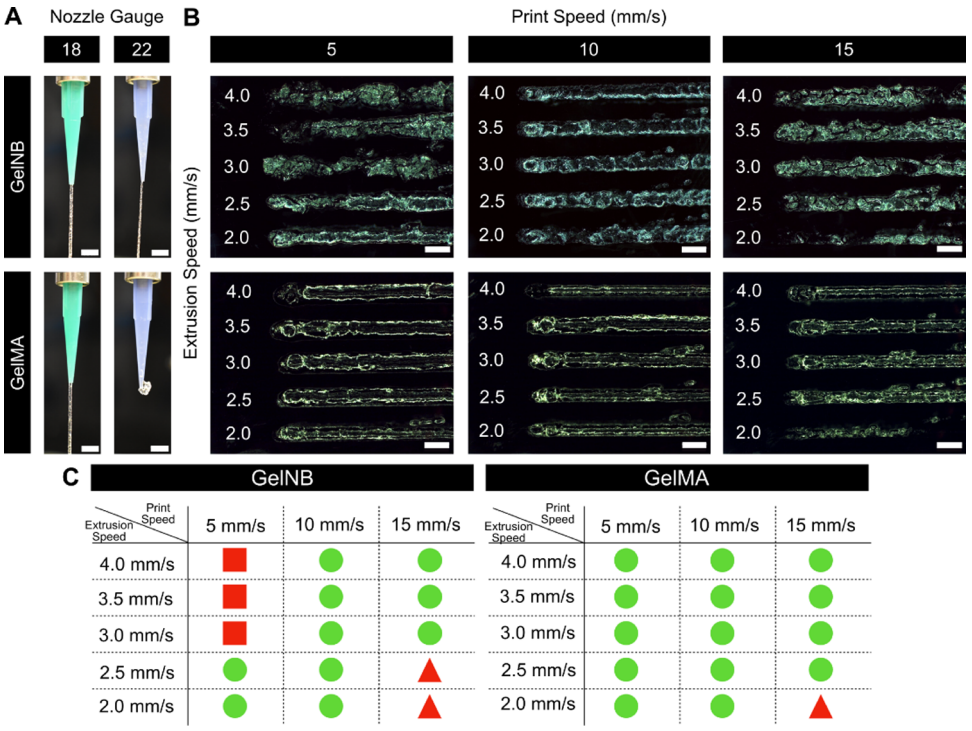

Figure 4. Assessment of extruded filament quality. (A) 10% GelNB and GelMA were extruded through 18 and 20 gauge nozzles to assess compatibility with different nozzle sizes. (B) Biomaterial inks were deposited at print speeds ranging from 5 to 15 mm s^{-1} and extrusion speeds ranging from 2.0 to 4.0 mm s^{-1} (28.51−57.01 μL s^{-1}), and filaments were qualitatively assessed. (C) Squares represent overextrusion, triangles represent underextrusion, and circles represent appropriate extrusion. Scale bars are (A) 5 mm and (B) 3 mm.

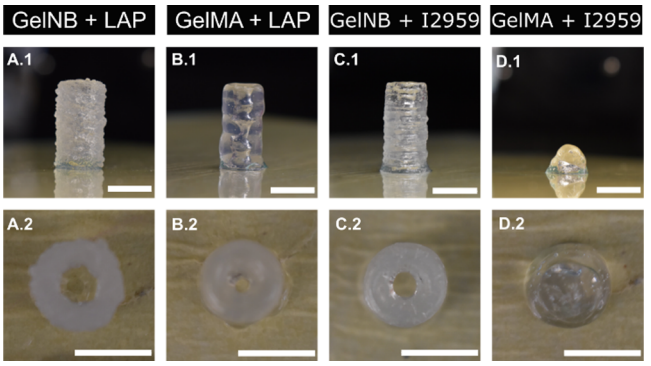

Figure 5. *Z* stability in printed constructs. Biomaterial inks were printed up to 20 mm in height as vertical-standing cylindrical constructs with stabilization from simultaneous photochemical cross-linking. *Z* stability was evaluated in constructs fabricated from (A) GelNB + LAP, (B) GelMA + LAP, (C) GelNB + I2959, and (D) GelMA + I2959. Scale bars are 10 mm.

Although comparative mechanistic and kinetic studies of GelNB and GelMA's temperature-dependent gelation should be further performed, their differences in physical gelation may be of interest when designing thermally gelling bioinks.[7,47] Biomaterial inks were then subjected to shear rate sweeps, which revealed modest shear-thinning character in all formulations as indicated by negative-trending power-law relationships between viscosity and shear rate (Figure 2B). Yielding and shear-thinning character were identified in all biomaterial ink formulations, supporting their application in bioink formulations.

During deposition, bioinks should quickly solidify to maintain construct fidelity and stability.[2] To achieve this, simultaneous chemical cross-linking has been applied to quickly develop bioink mechanical properties.[13] *In situ* UV-curing time sweeps were performed to assess the applicability of GelNB, GelMA, LAP, and I2959 to the design of bioinks intended to be photocured during deposition. Formulations containing LAP exhibited faster storage modulus evolution compared to formulation containing I2959 (Figure 3A vs Figure 3B). This was especially realized considering LAP formulations were exposed to 365 nm light at an intensity of 5 mW cm^{-2}, while I2959 formulations were exposed at an intensity of 15 mW cm^{-2}. Additionally, GelNB exhibited faster storage modulus evolution in I2959-initiated sweeps compared to GelMA (Figure 3B). This finding is in correspondence with a previous report.[27] However, any increase in storage modulus evolution associated with GelNB appeared to be overshadowed by the increase associated with LAP (Figure 3A.1). The first time derivative of the time sweeps better elucidated the differences in storage modulus evolution within LAP-initiated sweeps. GelNB + LAP exhibited a slightly greater peak rate change of storage modulus compared to GelMA + LAP (Figure 3A.2). Within I2959 initiated sweeps, GelNB exhibited a peak rate change of storage modulus about an order of magnitude greater than GelMA (Figure 3B.2). Thus, LAP greatly increased storage modulus evolution compared to I2959, and GelNB moderately increased storage modulus evolution compared to GelMA. These findings support the preferential inclusion of GelNB and LAP in bioinks intended to be photocured during fabrication.

Print Parameter Optimization. The extrusion character of bioinks can be adjusted by modifying print parameters such as nozzle shape and size, print speed, and extrusion speed.[7,22] Biomaterial inks were extruded through 18 gauge (838 μm i.d.) and 20 gauge (603 μm i.d.) tapered nozzles. The GelNB-

DOI: 10.1021/acs.biomac.9b01204
Biomacromolecules XXXX, XXX, XXX−XXX

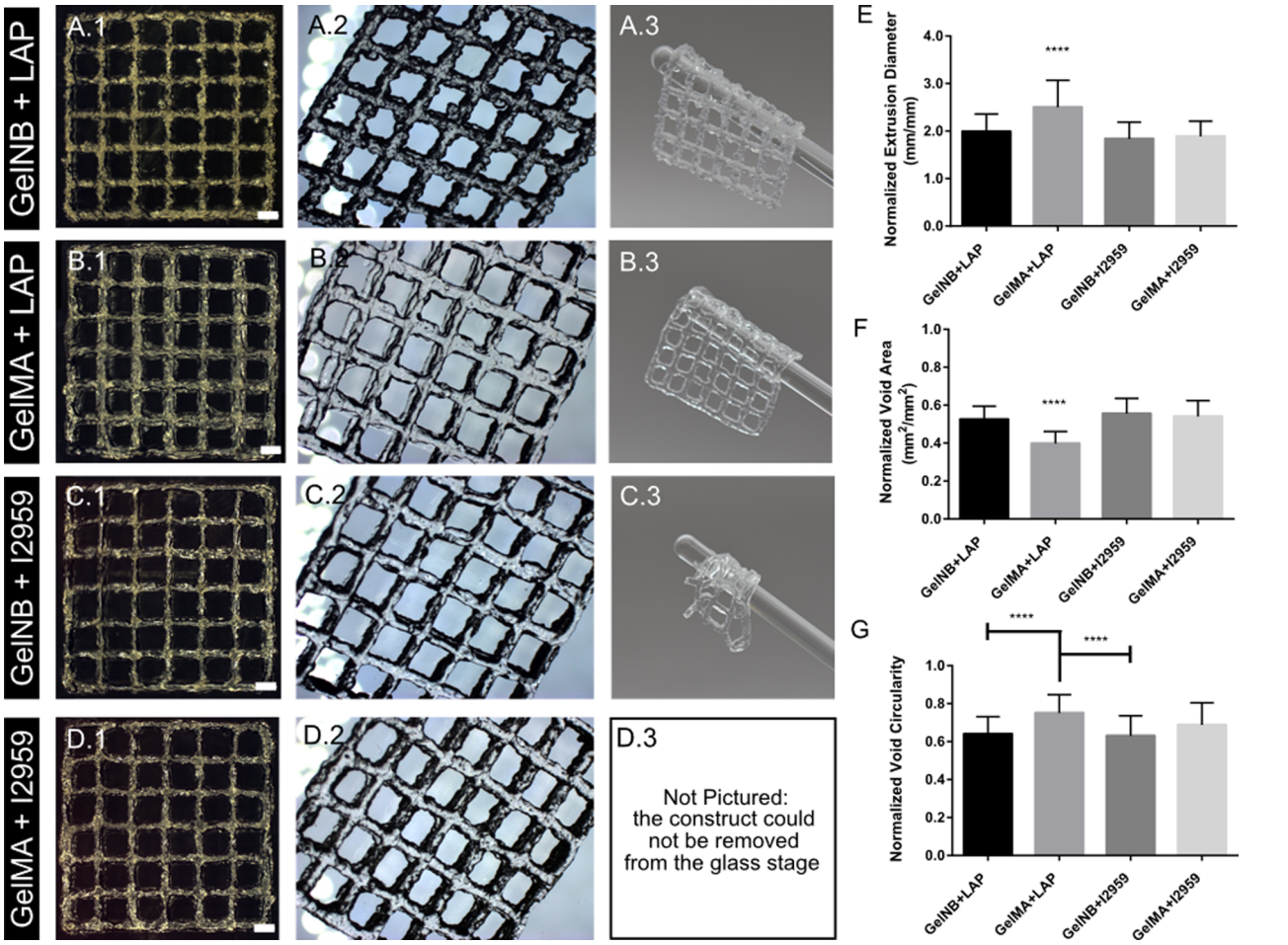

Figure 6. Filament spreading and $X-Y$ fidelity in printed constructs. (A.1−D.1) Grid constructs were printed to 1 mm in height from biomaterial ink formulations, (A.2−D.2) exhibiting variable surface roughness (A.3−D.3) and handleability. (E−G) Extrusion diameters, void areas, and void circularities were analyzed via image processing of (A.1−D.1) in ImageJ. Scale bars are 3 mm.

containing formulation formed a regular filament upon extrusion though both nozzle sizes, while the GelMA-containing formulation formed a regular filament only upon extrusion through the 18 gauge nozzle (Figure 4A). Subsequent experiments were conducted using an 18 gauge nozzle because of its compatibility with formulations containing either GelNB or GelMA. Next, biomaterial inks were deposited to one layer in height at print speeds of 5.0, 10.0, and 15.0 mm s^{-1} and five extrusion speeds ranging from 2.0 to 4.0 mm s^{-1} in increments of 0.5 mm s^{-1}. A qualitative description of deposited extrusion filament was recorded. The GelNB biomaterial ink was considered overextruded (exhibiting relatively large and heterogeneous extrusion diameters) at print speed:extrusion speed ratios less than 2.0 and underextruded (displaying relatively small extrusion diameters and discontinuities along stretches) at print speed:extrusion speed ratios greater than 5.0 (Figure 4B). The GelMA-containing formulation was considered underextruded for print speed:extrusion speed ratios greater than 6.0 and appropriately extrudable under all other investigated parameters (Figure 4B). The evaluation of biomaterial ink extrusion character was organized in Figure 4C. GelMA exhibited appropriate extrusion character over a wider range of print speed:extrusion speed ratios compared to GelNB. This result might be expected because GelMA biomaterial inks exhibited yielding to viscous flow in rheological sweeps at relatively lower shear stress (Figure 2A). In terms of bioink formulation, these results suggest 10% w/v GelMA can be more regularly extruded under a wider range of print parameters relative to 10% w/v GelNB.

Assessment of *Z* Stability. Photochemical cross-linking can be applied during deposition to solidify bioinks and preserve construct fidelity and stability.[13] To examine the dependence of construct stability on biomaterial ink formulation, constructs were printed up to 20 mm in height according to a vertical-cylinder CAD file and cured via continuous exposure to 365 nm light. Constructs fabricated from biomaterial inks containing GelMA exhibited stability upon UV curing with initiation mediated by LAP but instability and pooling upon UV curing initiated by I2959 (Figure 5B vs Figure 5D). The difference between the groups is further realized considering LAP formulations were exposed to 365 nm light at an intensity of 5 mW cm^{-2} while I2959 were exposed at an intensity of 20 mW cm^{-2}. This result supports the application of LAP in bioinks intended to be chemically cross-linked during deposition as opposed to I2959. Additionally, constructs exhibited stability when GelNB was substituted for GelMA in I2959 formulations (Figure 5C vs Figure 5D). This result is likely reflective of both greater mechanical properties prior to curing and increased chemical cross-linking kinetics during curing in GelNB biomaterial inks. While GelNB formulations exhibited stability regardless of photoinitiator identity, GelNB constructs exhibited greater surface roughness

DOI: 10.1021/acs.biomac.9b01204
Biomacromolecules XXXX, XXX, XXX−XXX

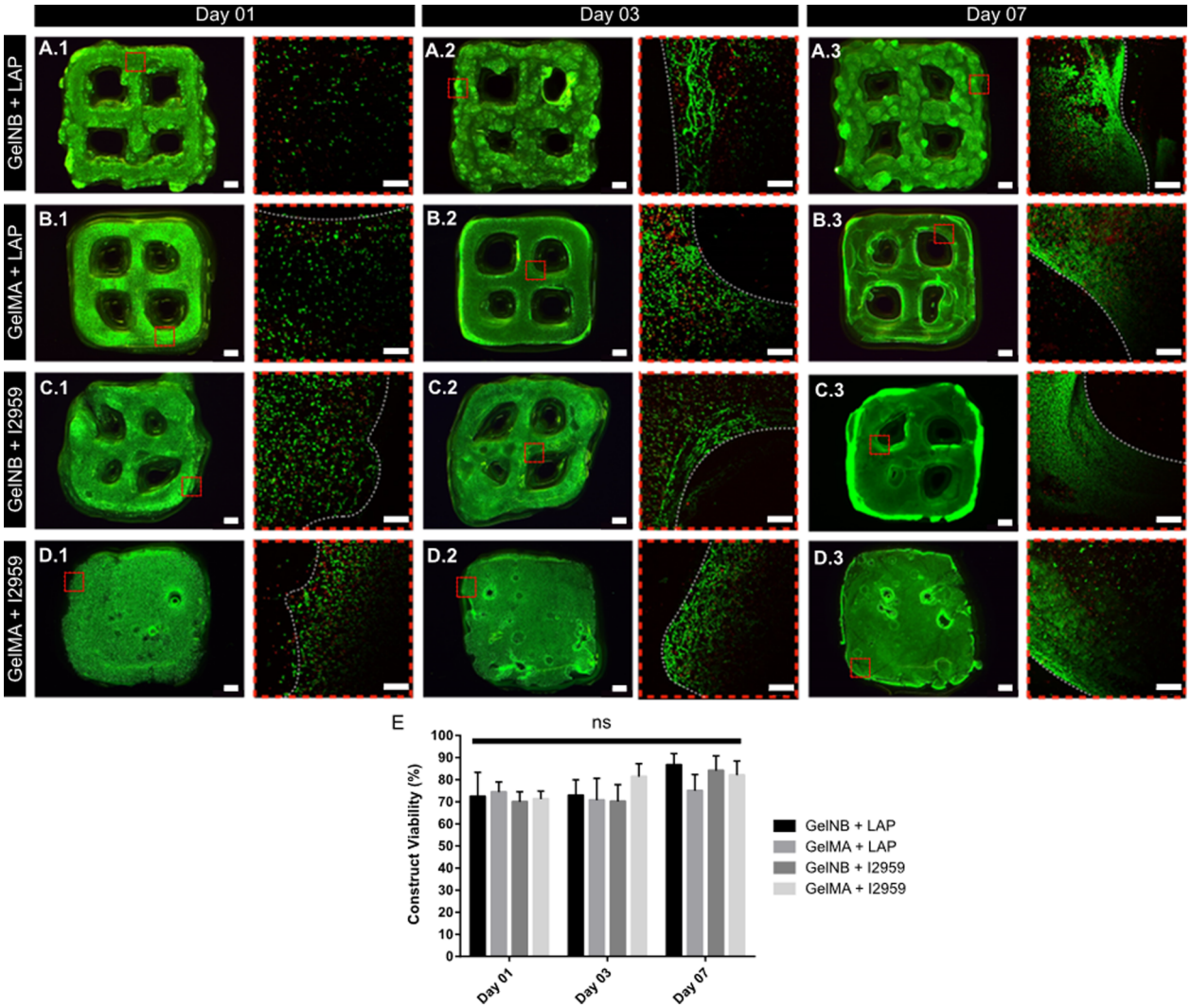

Figure 7. NIH 3T3 viability in printed constructs. (A−D) Grid constructs, fabricated from bioinks laden with NIH 3T3 fibroblasts, were subjected to viability staining on 1, 3, and 7 days of culture. (E) Live and dead cells were counted in ImageJ, and construct viabilities were calculated. Scale bars are 1000 μm by full constructs and 200 μm within insets.

and turbidity relative to GelMA constructs (Figure 5). This might be indicative of relatively turbulent flow during extrusion of GelNB formulations, which could result in the capture and retention of air bubbles. In regards to construct stability, these results support the selection of LAP and 10% w/v GelNB to the design of bioinks intended to be simultaneously printed and photocured opposed to I2959 and 10% w/v GelMA, respectively.

Assessment of *X*−*Y* Print Fidelity and Filament Spreading. Filament spreading upon bioink deposition results in decreased spatial fidelity in bioprinted constructs. To assess the dependence of construct *X*−*Y* fidelity on biomaterial ink formulation, constructs were printed in a 5 layered, six square by six square grid pattern and cured upon continuous exposure to 365 nm light. Images of the constructs on the glass collecting stage were taken on a stereomicroscope (Figure 6A.1−D.1). Tilting the glass stage showed construct three-dimensionality and surface roughness (Figure 6A.2−D.2). Images displayed in Figure 6A.2−D.2 were processed in ImageJ to evaluate extrusion diameter, void area, and void circularity. Interestingly, GelMA + LAP exhibited significantly increased extrusion diameter and void circularity and significantly decreased void area compared to other formulations (Figure 6E−G). These differences may be due to thermal hysteresis during biomaterial preparation. When preparing biomaterial inks, components were mixed at 40 °C and then allowed to physically gel at room temperature (22.5 °C) for about 20−60 min before loading into the printer's extruder. Although all formulations were necessarily gelled, GelMA + LAP may have formed a weaker physically cross-linked gel if it was not incubated at room temperature for as long as GelMA + I2959. Rheological evaluations of the physical gelation kinetics of GelMA biomaterial inks, which confirmed thermal and temporal dependence within the 20−60 min time range during incubation at room temperature (Figure S3), support this possibility. Printing mechanically weak biomaterial inks would be expected to correlate with greater filament spreading. Moreover, printing mechanically weak biomaterial inks would generate less turbulence during extrusion, resulting in decreased surface roughness and, potentially, improved void circularity compared to formulations containing GelNB (Figure 6G). Constructs were removed from the glass collection stage to evaluate construct handleability. LAP constructs retained shape upon handling

DOI: 10.1021/acs.biomac.9b01204
Biomacromolecules XXXX, XXX, XXX−XXX

(Figure 6A.3−B.3) while the GelNB + I2959 constructs tore along most filaments (Figure 6C.3), and the GelMA + I2959 constructs could not be removed from the stage without fully compromising shape fidelity (Figure 6D.3). These results indicated substantial cross-link conversion in LAP formulations, moderate cross-link conversion in GelNB + I2959, and low cross-link conversion in GelMA + I2959. In regards to *X*−*Y* fidelity, these results strongly support the selection of LAP over I2959 as a photoinitiator. The results also indicate similar *X*−*Y* fidelity between GelNB and GelMA, although roughness was increased with the GelNB bioink formulations.

Assessment of NIH 3T3 Viability in Bioprinted Constructs. The presence of encapsulated cells, which remodel bioprinted constructs through the secretion of proteolytic enzymes and extracellular matrix proteins, is a defining feature of 3D bioprinting and ultimately lends to the functional success of constructs. As such, bioprinted constructs should exhibit high cell viability following fabrication.[48] To assess the dependency of cell viability on bioink formulation, bioinks laden with NIH 3T3 fibroblasts were printed in a two square by two square grid pattern. The constructs were cultured under standard conditions and subjected to viability staining after 1, 3, and 7 days. Confocal fluorescence microscopy images of stained constructs qualitatively revealed relatively more live cells than dead cells in all formulations (Figure 7A−D). Cell numbers were counted in confocal images to provide a semiquantitative evaluation of viability. At all culture time points, all bioink formulations exhibited viabilities greater than about 70%. As culture time increased, cell viability in general increased, although no significant increases were detected between culture time points within individual bioink formulations. Interestingly, culture time points being equal, no significant differences were detected between bioink formulations (Figure 7E). Cell viability was expected to be detrimentally impacted in bioink formulations that exhibited relatively increased stress generation during extrusion,[3,19] increased nonspecific radical propagation,[35] and/or increased UV dosage required for acceptable curing.[6] The result most likely indicates that differences between formulations, in terms of the aforementioned bioink properties, are innocuous to cell viability in the employed system. In terms of cell viability, all of the investigated bioink components appear to be compatible with extrusion bioprinting. However, it is possible that differences in viability between chain growth and thiol−ene reactions might be observed when printing more sensitive cell types.

CONCLUSIONS

The ultimate goal of this work was to provide material recommendations for the formulation of extrudable gelatin-based bioinks by comparing GelNB and LAP to the more commonly used GelMA and I2959. NIH 3T3 cell viability was not influenced by the identity of the gelatin macromer or photoinitiator, despite differences in physical properties and applied UV dosage. However, several notable differences were found in studies assessing construct stability and fidelity. The presented data strongly support the preferential incorporation of LAP in bioink formulations as opposed to I2959, as LAP was shown to impart biomaterial inks with faster storage modulus evolution upon exposure to 365 nm light and to improve *Z* stability in printed constructs regardless of the gelatin derivative used. In terms of macromer composition, the data also support the use of GelNB in bioink formulations, which exhibited moderately faster storage modulus evolution and improved *Z* stability compared to GelMA bioinks. While formulations containing GelMA were found to yield at lower shear stresses, which translated to the deposition of filaments with less surface roughness at a wider range of print speeds and extrusion speeds, it should be noted that all experiments were performed with the same macromer concentration and at ambient temperature. Future studies should investigate optimization of GelNB concentration and extrusion temperature as well as photoinitiator concentration and UV light intensity.

ASSOCIATED CONTENT

Supporting Information

The Supporting Information is available free of charge at https://pubs.acs.org/doi/10.1021/acs.biomac.9b01204.

NMR spectra of functionalized gelatin derivatives and derivation of functionalization equations and extrusion speed equations (PDF)

AUTHOR INFORMATION

Corresponding Author

*E-mail: dalge@tamu.edu (D.L.A).

ORCID

Akhilesh K. Gaharwar: 0000-0002-0284-0201

Daniel L. Alge: 0000-0002-8129-2871

Funding

This research was supported by the National Science Foundation (CMMI 1634858 to D.L.A. and CBET 1705852 to A.K.G.), the National Institutes of Health (DP2 EB026265 to A.K.G.), and the College of Engineering at Texas A&M University (Engineering Graduate Merit Fellowship to T.J.T.).

Notes

The authors declare no competing financial interest.

ACKNOWLEDGMENTS

The authors acknowledge Texas A&M Microscopy and Imaging Center for providing access to the Olympus FV1000 confocal microscope and Shannon Mitchell Hair for his contribution in the circuit design of the custom UV-curing accessory.

ABBREVIATIONS

3D, three-dimensional; GelMA, gelatin−methacryloyl; GelNB, gelatin−norbornene; I2959, Irgacure D-2959, 2-hydroxy-4′-(2-hydroxyethoxy)-2-methylpropiophenone; LAP, lithium phenyl-2,4,6 trimethylbenzoylphosphinate.

REFERENCES

(1) Melchels, F. P. W.; Domingos, M. A. N.; Klein, T. J.; Malda, J.; Bartolo, P. J.; Hutmacher, D. W. Additive manufacturing of tissues and organs. *Prog. Polym. Sci.* **2012**, *37* (8), 1079−1104.

(2) Murphy, S. V.; Atala, A. 3D bioprinting of tissues and organs. *Nat. Biotechnol.* **2014**, *32*, 773.

(3) Holzl, K.; Lin, S.; Tytgat, L.; Van Vlierberghe, S.; Gu, L.; Ovsianikov, A. Bioink properties before, during and after 3D bioprinting. *Biofabrication* **2016**, *8* (3), 032002.

(4) Liu, Y.; Chan-Park, M. B. A biomimetic hydrogel based on methacrylated dextran-graft-lysine and gelatin for 3D smooth muscle cell culture. *Biomaterials* **2010**, *31* (6), 1158−1170.

(5) Schuurman, W.; Levett, P. A.; Pot, M. W.; van Weeren, P. R.; Dhert, W. J.; Hutmacher, D. W.; Melchels, F. P.; Klein, T. J.; Malda, J.

DOI: 10.1021/acs.biomac.9b01204
Biomacromolecules XXXX, XXX, XXX−XXX

Gelatin-methacrylamide hydrogels as potential biomaterials for fabrication of tissue-engineered cartilage constructs. *Macromol. Biosci.* **2013**, *13* (5), 551−61.
(6) Bertassoni, L. E.; Cardoso, J. C.; Manoharan, V.; Cristino, A. L.; Bhise, N. S.; Araujo, W. A.; Zorlutuna, P.; Vrana, N. E.; Ghaemmaghami, A. M.; Dokmeci, M. R.; Khademhosseini, A. Direct-write bioprinting of cell-laden methacrylated gelatin hydrogels. *Biofabrication* **2014**, *6* (2), 024105.
(7) Liu, W.; Heinrich, M. A.; Zhou, Y.; Akpek, A.; Hu, N.; Liu, X.; Guan, X.; Zhong, Z.; Jin, X.; Khademhosseini, A.; Zhang, Y. S. Extrusion Bioprinting of Shear-Thinning Gelatin Methacryloyl Bioinks. *Adv. Healthcare Mater.* **2017**, DOI: 10.1002/adhm.201770062.
(8) Yue, K.; Trujillo-de Santiago, G.; Alvarez, M. M.; Tamayol, A.; Annabi, N.; Khademhosseini, A. Synthesis, properties, and biomedical applications of gelatin methacryloyl (GelMA) hydrogels. *Biomaterials* **2015**, *73*, 254−271.
(9) Emsley, J.; Knight, C. G.; Farndale, R. W.; Barnes, M. J.; Liddington, R. C. Structural Basis of Collagen Recognition by Integrin $\alpha 2\beta 1$. *Cell* **2000**, *101* (1), 47−56.
(10) Nichol, J. W.; Koshy, S. T.; Bae, H.; Hwang, C. M.; Yamanlar, S.; Khademhosseini, A. Cell-laden microengineered gelatin methacrylate hydrogels. *Biomaterials* **2010**, *31* (21), 5536−44.
(11) Van Den Bulcke, A. I.; Bogdanov, B.; De Rooze, N.; Schacht, E. H.; Cornelissen, M.; Berghmans, H. Structural and Rheological Properties of Methacrylamide Modified Gelatin Hydrogels. *Biomacromolecules* **2000**, *1* (1), 31−38.
(12) Ouyang, L.; Highley, C. B.; Sun, W.; Burdick, J. A. A Generalizable Strategy for the 3D Bioprinting of Hydrogels from Nonviscous Photo-crosslinkable Inks. *Adv. Mater.* **2017**, *29* (8), 1604983.
(13) Hockaday, L. A.; Kang, K. H.; Colangelo, N. W.; Cheung, P. Y.; Duan, B.; Malone, E.; Wu, J.; Girardi, L. N.; Bonassar, L. J.; Lipson, H.; Chu, C. C.; Butcher, J. T. Rapid 3D printing of anatomically accurate and mechanically heterogeneous aortic valve hydrogel scaffolds. *Biofabrication* **2012**, *4* (3), 035005.
(14) Lee, B. H.; Lum, N.; Seow, L. Y.; Lim, P. Q.; Tan, L. P. Synthesis and Characterization of Types A and B Gelatin Methacryloyl for Bioink Applications. *Materials* **2016**, *9* (10), 797.
(15) Decker, C.; Jenkins, A. D. Kinetic approach of oxygen inhibition in ultraviolet- and laser-induced polymerizations. *Macromolecules* **1985**, *18* (6), 1241−1244.
(16) O'Connell, C. D.; Zhang, B.; Onofrillo, C.; Duchi, S.; Blanchard, R.; Quigley, A.; Bourke, J.; Gambhir, S.; Kapsa, R.; Di Bella, C.; Choong, P.; Wallace, G. G. Tailoring the mechanical properties of gelatin methacryloyl hydrogels through manipulation of the photocrosslinking conditions. *Soft Matter* **2018**, *14* (11), 2142−2151.
(17) de Gruijl, F. R.; Sterenborg, H. J. C. M.; Forbes, P. D.; Davies, R. E.; Cole, C.; Kelfkens, G.; van Weelden, H.; Slaper, H.; van der Leun, J. C. Wavelength Dependence of Skin Cancer Induction by Ultraviolet Irradiation of Albino Hairless Mice. *Cancer Res.* **1993**, *53* (1), 53.
(18) Svobodová, A. R.; Galandáková, A.; Šianská, J.; Doležal, D.; Lichnovská, R.; Ulrichová, J.; Vostálová, J. DNA damage after acute exposure of mice skin to physiological doses of UVB and UVA light. *Arch. Dermatol. Res.* **2012**, *304* (5), 407−412.
(19) Ouyang, L.; Yao, R.; Zhao, Y.; Sun, W. Effect of bioink properties on printability and cell viability for 3D bioplotting of embryonic stem cells. *Biofabrication* **2016**, *8* (3), 035020.
(20) Klotz, B. J.; Gawlitta, D.; Rosenberg, A. J. W. P.; Malda, J.; Melchels, F. P. W. Gelatin-Methacryloyl Hydrogels: Towards Biofabrication-Based Tissue Repair. *Trends Biotechnol.* **2016**, *34* (5), 394−407.
(21) Ouyang, L.; Highley, C. B.; Rodell, C. B.; Sun, W.; Burdick, J. A. 3D Printing of Shear-Thinning Hyaluronic Acid Hydrogels with Secondary Cross-Linking. *ACS Biomater. Sci. Eng.* **2016**, *2* (10), 1743−1751.
(22) Gao, Q.; Niu, X.; Shao, L.; Zhou, L.; Lin, Z.; Sun, A.; Fu, J.; Chen, Z.; Hu, J.; Liu, Y.; He, Y. 3D printing of complex GelMA-based scaffolds with nanoclay. *Biofabrication* **2019**, *11* (3), 035006.
(23) Chimene, D.; Peak, C. W.; Gentry, J. L.; Carrow, J. K.; Cross, L. M.; Mondragon, E.; Cardoso, G. B.; Kaunas, R.; Gaharwar, A. K. Nanoengineered Ionic−Covalent Entanglement (NICE) Bioinks for 3D Bioprinting. *ACS Appl. Mater. Interfaces* **2018**, *10* (12), 9957−9968.
(24) Suntornnond, R.; Tan, E. Y. S.; An, J.; Chua, C. K. A highly printable and biocompatible hydrogel composite for direct printing of soft and perfusable vasculature-like structures. *Sci. Rep.* **2017**, *7* (1), 16902.
(25) Mũnoz, Z.; Shih, H.; Lin, C.-C. Gelatin hydrogels formed by orthogonal thiol−norbornene photochemistry for cell encapsulation. *Biomater. Sci.* **2014**, *2* (8), 1063−1072.
(26) Koshy, S. T.; Desai, R. M.; Joly, P.; Li, J.; Bagrodia, R. K.; Lewin, S. A.; Joshi, N. S.; Mooney, D. J. Click-Crosslinked Injectable Gelatin Hydrogels. *Adv. Healthcare Mater.* **2016**, *5* (5), 541−547.
(27) Van Hoorick, J.; Gruber, P.; Markovic, M.; Rollot, M.; Graulus, G.-J.; Vagenende, M.; Tromayer, M.; Van Erps, J.; Thienpont, H.; Martins, J. C.; Baudis, S.; Ovsianikov, A.; Dubruel, P.; Van Vlierberghe, S. Highly Reactive Thiol-Norbornene Photo-Click Hydrogels: Toward Improved Processability. *Macromol. Rapid Commun.* **2018**, *39* (14), 1800181.
(28) Tytgat, L.; Van Damme, L.; Van Hoorick, J.; Declercq, H.; Thienpont, H.; Ottevaere, H.; Blondeel, P.; Dubruel, P.; Van Vlierberghe, S. Additive manufacturing of photo-crosslinked gelatin scaffolds for adipose tissue engineering. *Acta Biomater.* **2019**, *94*, 340−350.
(29) Dobos, A.; Van Hoorick, J.; Steiger, W.; Gruber, P.; Markovic, M.; Andriotis, O. G.; Rohatschek, A.; Dubruel, P.; Thurner, P. J.; Van Vlierberghe, S.; Baudis, S.; Ovsianikov, A. Thiol−Gelatin−Norbornene Bioink for Laser-Based High-Definition Bioprinting. *Adv. Healthcare Mater.* **2019**, *0* (0), 1900752.
(30) Hoyle, C. E.; Lee, T. Y.; Roper, T. Thiol−enes: Chemistry of the past with promise for the future. *J. Polym. Sci., Part A: Polym. Chem.* **2004**, *42* (21), 5301−5338.
(31) Fairbanks, B. D.; Love, D. M.; Bowman, C. N. Efficient Polymer-Polymer Conjugation via Thiol-ene Click Reaction. *Macromol. Chem. Phys.* **2017**, *218* (18), 1700073.
(32) Fairbanks, B. D.; Schwartz, M. P.; Halevi, A. E.; Nuttelman, C. R.; Bowman, C. N.; Anseth, K. S. A Versatile Synthetic Extracellular Matrix Mimic via Thiol-Norbornene Photopolymerization. *Adv. Mater.* **2009**, *21* (48), 5005−5010.
(33) Ooi, H. W.; Mota, C.; ten Cate, A. T.; Calore, A.; Moroni, L.; Baker, M. B. Thiol−Ene Alginate Hydrogels as Versatile Bioinks for Bioprinting. *Biomacromolecules* **2018**, *19* (8), 3390−3400.
(34) Pereira, R. F.; Barrias, C. C.; Bártolo, P. J.; Granja, P. L. Cell-instructive pectin hydrogels crosslinked via thiol-norbornene photo-click chemistry for skin tissue engineering. *Acta Biomater.* **2018**, *66*, 282−293.
(35) Shubin, A. D.; Felong, T. J.; Graunke, D.; Ovitt, C. E.; Benoit, D. S. Development of poly(ethylene glycol) hydrogels for salivary gland tissue engineering applications. *Tissue Eng., Part A* **2015**, *21* (11−12), 1733−51.
(36) Lin, C.-C.; Raza, A.; Shih, H. PEG hydrogels formed by thiol-ene photo-click chemistry and their effect on the formation and recovery of insulin-secreting cell spheroids. *Biomaterials* **2011**, *32* (36), 9685−9695.
(37) Roberts, J. J.; Bryant, S. J. Comparison of photopolymerizable thiol-ene PEG and acrylate-based PEG hydrogels for cartilage development. *Biomaterials* **2013**, *34* (38), 9969−9979.
(38) Tibbitt, M. W.; Kloxin, A. M.; Sawicki, L.; Anseth, K. S. Mechanical Properties and Degradation of Chain and Step Polymerized Photodegradable Hydrogels. *Macromolecules* **2013**, *46* (7), 2785−2792.
(39) Bryant, S. J.; Nuttelman, C. R.; Anseth, K. S. Cytocompatibility of UV and visible light photoinitiating systems on cultured NIH/3T3 fibroblasts in vitro. *J. Biomater. Sci., Polym. Ed.* **2000**, *11* (5), 439−57.

DOI: 10.1021/acs.biomac.9b01204
Biomacromolecules XXXX, XXX, XXX−XXX

(40) Williams, C. G.; Malik, A. N.; Kim, T. K.; Manson, P. N.; Elisseeff, J. H. Variable cytocompatibility of six cell lines with photoinitiators used for polymerizing hydrogels and cell encapsulation. *Biomaterials* **2005**, *26* (11), 1211−1218.
(41) Fairbanks, B. D.; Schwartz, M. P.; Bowman, C. N.; Anseth, K. S. Photoinitiated polymerization of PEG-diacrylate with lithium phenyl-2,4,6-trimethylbenzoylphosphinate: polymerization rate and cytocompatibility. *Biomaterials* **2009**, *30* (35), 6702−7.
(42) Truong, V. X.; Hun, M. L.; Li, F.; Chidgey, A. P.; Forsythe, J. S. In situ-forming click-crosslinked gelatin based hydrogels for 3D culture of thymic epithelial cells. *Biomater. Sci.* **2016**, *4* (7), 1123−31.
(43) Shirahama, H.; Lee, B. H.; Tan, L. P.; Cho, N.-J. Precise Tuning of Facile One-Pot Gelatin Methacryloyl (GelMA) Synthesis. *Sci. Rep.* **2016**, *6*, 31036.
(44) Claaßen, C.; Claaßen, M. H.; Truffault, V.; Sewald, L.; Tovar, G. E. M.; Borchers, K.; Southan, A. Quantification of Substitution of Gelatin Methacryloyl: Best Practice and Current Pitfalls. *Biomacromolecules* **2018**, *19* (1), 42−52.
(45) Mouser, V. H.; Melchels, F. P.; Visser, J.; Dhert, W. J.; Gawlitta, D.; Malda, J. Yield stress determines bioprintability of hydrogels based on gelatin-methacryloyl and gellan gum for cartilage bioprinting. *Biofabrication* **2016**, *8* (3), 035003.
(46) Chattopadhyay, S.; Raines, R. T. Review collagen-based biomaterials for wound healing. *Biopolymers* **2014**, *101* (8), 821−833.
(47) Yin, J.; Yan, M.; Wang, Y.; Fu, J.; Suo, H. 3D Bioprinting of Low-Concentration Cell-Laden Gelatin Methacrylate (GelMA) Bioinks with a Two-Step Cross-linking Strategy. *ACS Appl. Mater. Interfaces* **2018**, *10* (8), 6849−6857.
(48) Skardal, A.; Devarasetty, M.; Kang, H.-W.; Mead, I.; Bishop, C.; Shupe, T.; Lee, S. J.; Jackson, J.; Yoo, J.; Soker, S.; Atala, A. A hydrogel bioink toolkit for mimicking native tissue biochemical and mechanical properties in bioprinted tissue constructs. *Acta Biomater.* **2015**, *25*, 24−34.

DOI: 10.1021/acs.biomac.9b01204
Biomacromolecules XXXX, XXX, XXX−XXX